

ICP-based SLAM Using LiDAR Intensity and Near-infrared Data *

Ryosuke Kataoka¹, Ryuki Suzuki¹, Yonghoon Ji², *Member, IEEE*, Hiromitsu Fujii³, *Member, IEEE*,
Hitoshi Kono⁴, *Member, IEEE*, and Kazunori Umeda¹, *Member, IEEE*

Abstract—Scan-matching is a method of localization based on the alignment of point clouds measured by sensors such as LiDAR. Most of the scan-matching methods utilize only the shape information of the point cloud. However, depending on the environment, features may not be sufficiently available from the shape information, and the accuracy of alignment may decrease. Therefore, we propose a highly accurate scan-matching method by using sensor fusion to obtain shape and physical features from the environment together. In this paper, the near-infrared information of water puddles, which is often seen inside the damaged nuclear power plant, and the reflection intensity of LiDAR are measured and utilized for localization. Experiment results in the real environment show that the proposed method improved the accuracy of the map and the trajectory of the robot by taking advantage of physical features observed from the environment.

I. INTRODUCTION

In the decommissioning activities using robots at the Fukushima Daiichi Nuclear Power Plant, which was damaged by 2011 Tohoku earthquake and tsunami. There were many accidents and failures of the robot system inside the nuclear power plant building, and the reason for this is thought of not enough information about the damage of the building. Therefore, it is necessary to accurately understand the state of the environment by generating a map of inside the building.

The generation of environmental maps is one of the most important methods for understanding the situation, and SLAM (simultaneous localization and mapping) systems using features have been extensively studied for generating feature-based environmental maps. Among them, SLAM with laser scan matching is widely used. ICP (iterative closest point) [1] is a traditional scan-matching method. There are many ICP derivatives [2-3] because of its extensibility. Similarly, in this paper, the scan matching is improved by adding a process that takes physical features into account to ICP. While many SLAM schemes use geometric information of the environment as features, there are also many examples of SLAM methods

that use features extracted from images captured by a camera [4-6]. However, a camera is not suitable for measuring dark environments such as inside the damaged nuclear plants, while LiDAR can easily obtain 3D shape of these environment. Rusu et al. used normal information extracted from point clouds as features [7]. However, this method cannot take advantage of many physical features inside the damaged plant. Inside the damaged nuclear power plant, there are a lot of physical quantities that are not often found in general environments: water puddle, heat source by the explosion, and radiation. Thus, these can be used as features in alignment of point clouds. There are several studies that make use of environmental features in SLAM. Hara et al. improved the scan matching by taking advantage of that the intensity of laser reflection from LiDAR depends on inherent reflective properties of materials [8]. Godin et al. used color features from color images to align point clouds [9]. However, these studies use a single sensor to acquire physical features, which leads to limitation of information acquisition. Hence, our method fuses LiDAR with other sensors to acquire features, which may be suitable for SLAM using many physical features in the damaged plant. In our previous work [10, 11], we proposed a SLAM that utilizes physical feature, but these values were virtually assigned due to difficulty of measuring point clouds that have information on physical feature values. On the other hand, in this paper, we integrate the proposed scan-matching method with the system for measuring actual near-infrared and LiDAR intensity.

In this paper, we propose a scan matching-based mapping system using reflection intensity of LiDAR and water puddles in a nuclear power plant as environmental features. Location of water puddle is estimated by near-infrared camera. Furthermore, by adding environmental features to the map generated by the proposed method, we can visualize water puddles as a hazardous area; thus, the map can be used as a simulation environment to plan the exploration of the buildings.

II. POINT CLOUD WITH PHYSICAL FEATURES

A. Physical Features in Environment

In this paper, physical information of the environment is used as features for alignment. LiDAR is capable of measuring various types of physical information more than just 3D shape and reflection intensity by combining with other sensors. For example, when an optical camera, a thermal camera, and a gamma camera are respectively combined, it is possible to obtain information on environmental features such as color,

*This work was founded by The Japan Atomic Energy Agency (JAEA) FY2020 Center of World Intelligence Project for Nuclear Science/Technology and Human Resource Development (Grant no. R02I015).

¹Course of Precision Engineering, Chuo University, 1-13-27 Kasuga, Bunkyo, Tokyo, Japan (e-mail: kataoka@sensor.mech.chuo-u.ac.jp)

²Graduate School for Advanced Science and Technology, Japan Advanced Institute of Science and Technology, 1-1 Asahidai, Nomi, Ishikawa, Japan

³Department of Advanced Robotics, Chiba Institute of Technology, 2-17-1 Thudanuma, Narashino-shi, Chiba, Japan

⁴Department of Engineering, Tokyo Polytechnic University, 1583 Iiyama, Atsugi, Kanagawa, Japan

heat source, and the radiation source, respectively. Water puddles exist inside the damaged nuclear power plant due to submersion caused by the accidents, and this information can be utilized as features in SLAM. Fujii et al. used a sensor system combining a near-infrared camera and RGB-D camera to generate point clouds with near-infrared information and visualize the transparent water puddles [12]. We incorporate LiDAR into the abovementioned sensor system to acquire point clouds with laser intensity and near-infrared information. Therefore, a single point in the point cloud has two variables in addition to the position information (x, y, z) : near-infrared intensity I_{IR} and LiDAR intensity I_{Laser} , and these two features are taken into account to improve the accuracy of mapping. Figure 1 shows experimental equipment used in this paper. Figure 2 shows point clouds with physical features obtained by measuring the artificial water puddle at the locations as shown in Fig. 1. Here, point clouds around the puddle is blue because that has low intensity of near-infrared. Note that the values of the near-infrared intensity have not been normalized to consider the distance to the observed object and the incidence of angle.

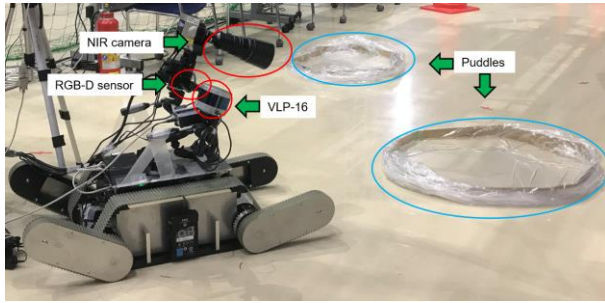


Fig. 1 Experimental equipment and artificial water puddles.

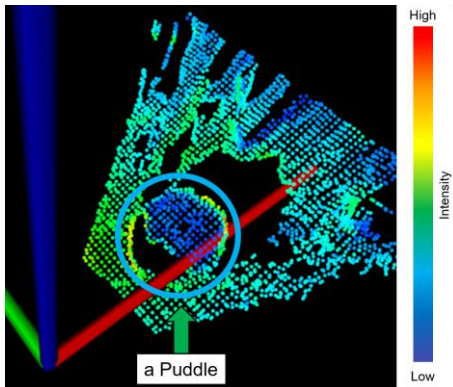


Fig. 2 Point clouds with physical features.

B. Classification of Point Clouds by Physical Features

We binarize the physical feature values of the points, which were continuous value, and divide the points into several classes before aligning them in order to perform the appropriate calculation for each class in our method. The point clouds are divided into four classes according to the value of near-infrared intensity and LiDAR intensity as shown in Table 1.

Table 1 Classification by physical feature values

	High near-infrared intensity I_{IR}	Low near-infrared intensity I_{IR}
High LiDAR intensity I_{Laser}	Class i	Class ii
Low LiDAR intensity I_{Laser}	Class iii	Class iv

III. ICP-SLAM WITH PHYSICAL FEATURES

A. Proposed System Overview

An overview of the proposed system is shown in Fig. 3. First, the robot remotely explores the environment and acquires point clouds (x, y, z) with physical features (I_{IR}, I_{Laser}) at each frame for generating a 3D map. Then, we perform global alignment to the point clouds in $t - 1$ frame and t frame by SAC-IA [6] using FPFH [6] features as initial alignment. SAC-IA uses only the shape information of the point clouds and does not consider I_{IR} and I_{Laser} . Here, an initial alignment is often given by odometry; however, the robot used in experiments has crawler type wheels and the error of odometry is large. Thus, we adopt global alignment instead of odometry. Moreover, scan-matching is performed by ICP with physical features to compute the rotation matrix \mathbf{R} and the translation vector \mathbf{T} , which are the parameters of rigid transformation to align the point clouds in each frame. Compared with conventional ICP, incorrect correspondences of points can be avoided by considering physical information. In ICP with physical features, as mentioned in Section II, we divide the measured point clouds with physical features into several classes, then improve the alignment by modifying a nearest neighbor search process according to the size of these classes. By calculating \mathbf{R} and \mathbf{T} at each frame, the position of robot is sequentially localized and its trajectory is calculated. However, this trajectory may have accumulated errors by scan matching; thus, we apply a pose adjustment to the trajectory. Pose adjustment is widely used to reduce the accumulated scan matching errors. Finally, the map with point clouds is generated by performing rigid transformation to the point clouds in each frame according to the trajectory optimized by the pose adjustment.

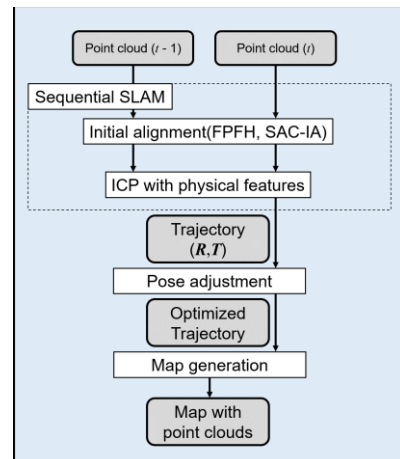


Fig. 3 System overview.

B. Conventional ICP Algorithm

In this paper, we propose a method based on the ICP algorithm, which is mainly used in scan-matching-based SLAM. Therefore, we briefly describe the conventional ICP algorithm in this subsection. First, we set the initial positions of each point clouds for alignment. This is to avoid the loss of accuracy and increase in computational cost caused by the distance between the point clouds. In SLAM of a mobile robot, the predicted state of the mobile robot in odometry is generally set as the initial position. Then, we solve a minimization problem that evaluates the alignment state by summing the distances between the points. At this time, we align the points scanned in the current frame (i.e., source point cloud), with the points scanned in the previous frame (i.e., target point cloud). In alignment, the rotation matrix \mathbf{R} and the translation vector \mathbf{T} , which represent the rigid transformation, are calculated by iterating the nearest neighbor search and the transformation matrix calculation using the sum of the squared distance E as the evaluated value, as written in the following equation.

$$E = \sum_{i=1}^N |\mathbf{p}_{k_i} - (\mathbf{q}_i \mathbf{R} + \mathbf{T})|^2 \quad (1)$$

- E : sum of the squared distance (i.e., evaluation value)
- \mathbf{p} : a point in the source point cloud
- \mathbf{q} : a point in the target point cloud
- N : the number of a points in the source point cloud (i.e., number of iterations)
- k_i : the reference scan data point corresponding to the point i in the source point cloud
- \mathbf{R} : the rotation matrix
- \mathbf{T} : the translation vector

C. ICP Algorithm with Physical Features

In this subsection, we describe the ICP algorithm with physical features proposed in our previous work [10]. Although the computation of the rigid transformation is the same as the conventional ICP, we can improve the alignment results by taking the physical features of points into account during the nearest neighbor search. As mentioned in Section II, we divide the measured point clouds with physical features into four classes. Here, we call the class with the relatively small number of points the “rare class”. In the nearest neighbor search, the accuracy of matching can be improved by expanding the search area when the query point belongs to the rare class. The points of the rare class are considered to be existing only in a limited area of the environment. Therefore, if we preferentially match points of the same rare class with each other, they are likely to be measured from the same location in the environment. On the other hand, there is a disadvantage that the same class of the rare class is difficult to match with each other in a common nearest neighbor search because they are located only in a limited area of the environment. Therefore, we can deal with this problem by expanding the search area of the nearest neighbor search of the points of the rare class to increase the probability of matching with points of the same class. In addition, by giving a penalty

α to the evaluation value of the nearest neighbor search in the ICP, points belonging to the same class are preferentially paired each other as shown in Fig. 4(b), which improves the accuracy of alignment. On the other hand, in ICP, if the shapes of the point clouds are similar, they will be attracted to each other despite their wrong matching, which may cause alignment failure as shown in Fig. 4(a). In this paper, we align point clouds with considering the physical feature values measured from the actual environment by using the measurement system described in Section II. The sum of the squared distances E between the nearest neighboring points can be represented as follows.

$$E = \sum_{i=1}^N |\mathbf{p}_{k_i} - (\mathbf{q}_i \mathbf{R} + \mathbf{T})|^2 + \lambda(\mathbf{p}_{k_i}, \mathbf{q}_i) \quad (2)$$

$$\lambda(\mathbf{p}, \mathbf{q}) = \begin{cases} \alpha & \text{if } c(\mathbf{p}) \neq c(\mathbf{q}) \\ 0 & \text{if } c(\mathbf{p}) = c(\mathbf{q}) \end{cases}$$

- $c(\mathbf{p})$: the class of the point \mathbf{p} considering its physical feature value

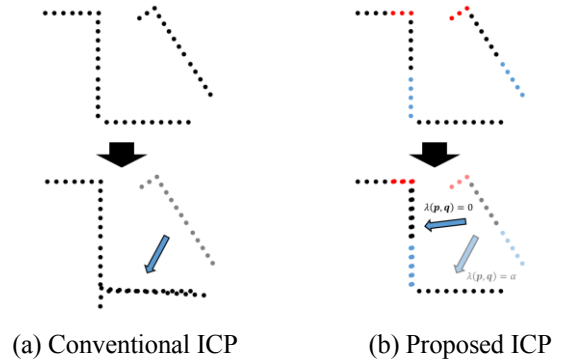


Fig. 4 Conceptual image of ICP algorithm.

IV. EXPERIMENT

A. Overview

We generated the map from point clouds with physical features measured by the sensor system consisting of a near-infrared camera, an RGB-D sensor, and a LiDAR. The sensor system is installed on the robot to measure the environment while moving it by remote control. The experiments were conducted in the test building of the Naraha Center for Remote Control Technology Development shown in Fig. 5. This facility is suitable for conducting ICP-SLAM evaluation experiments because it is rich in buildings with characteristic shapes such as mock-up stairs. The example of robot movement in the environment is shown in Fig. 6. Figure 8 shows the true map generated by using the true robot trajectory. Note that the true robot trajectory is calculated by the rigid body transformations obtained by manual alignment of point clouds. In order to reproduce the water-rich environment, artificial puddles were installed in the environment as shown in Fig. 1. The puddle is located at the sky-blue ellipses in Figs. 5, 8, and 9. Here, Fig. 8 shows expanded view of the area of the yellow box in Fig. 7. In Fig. 7, the purple line is the trajectory of the robot. As a result of classifying the point

clouds from all measured frames according to Table 1, class i and class iv are the rare classes described in ICP algorithm because the number of points that belong to these classes is relatively smaller than one of other classes. In Fig. 7, in order to make the points of the rare class more visible, we represent the points of class i, class iv, and the other classes, as red, blue, and white colors, respectively.



Fig. 5 Bird's-eye view of the experimental environment.

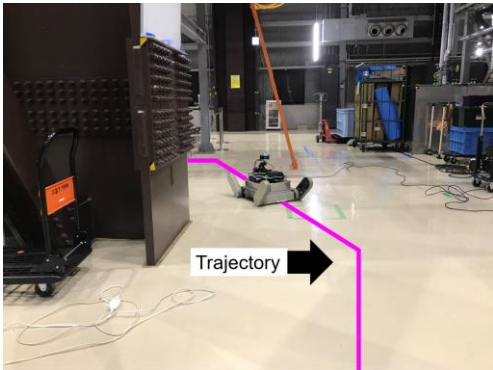


Fig. 6 Example robot movement in environment.

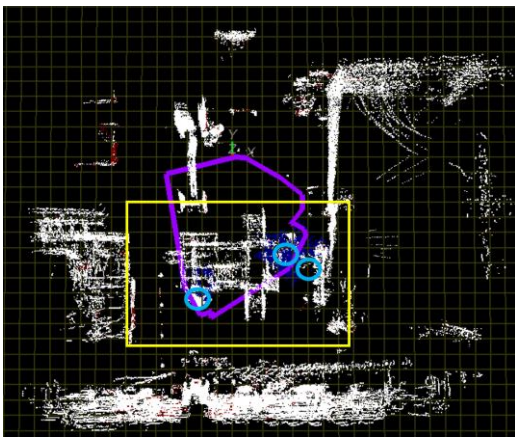


Fig. 7 Map built by true trajectory.

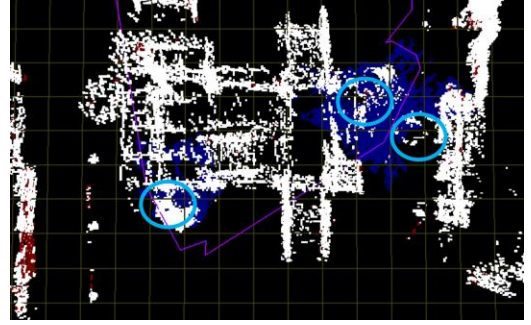


Fig. 8 Expanded view of true map.

B. Experimental equipment

Figure 1 shows experimental equipment used in this paper. The specifications of the robot are shown in Table 2. The robot is equipped with LiDAR sensor, a near-infrared camera, and an RGB-D sensor. We used a Velodyne LiDAR VLP-16 as the LiDAR sensor. This LiDAR can acquire 3D point clouds and laser reflection intensity of the environment. A near-infrared lens (Kowa LM8HC-SW) and a teleconversion lens (Raynox DCR-2025PRO) were attached to the near-infrared camera (BITRAN BK51-IGA). An Intel RealSense D415 was used for RGB-D sensor. More detailed description of the sensor system is described in [12]. Here, the sensors are fixed to each other and the relative position of the measured data is known.

Table 2 Specification of exploration robot

Uphill slope angle [deg]	45
Payload [kg]	5
Traveling speed [mm/s]	100
Length [mm]	1000
Width [mm]	400
Height [mm]	200

C. Experimental result

To verify the effectiveness of the proposed method, comparative experiments were conducted. We conducted experiments under the same conditions using two different methods: SLAM based on ICP described in subsection III.B, and SLAM based on extended ICP described in Fig. 3 and subsection III.C. The results shown in Fig. 9 and Table 3 show that the translation error of the robot position reduced by the proposed method. In addition, as shown in Fig. 10 and Table 4, the accuracy of the map was improved when the proposed method is used. Table 4 shows mean of the position errors of the points of the generated map. However, while the trajectory and map generated are better than those of the conventional method, the accuracy is still not as good as the true map shown in Fig. 7. One possible reason for this is that the measured area often changed depending on the frame.

This makes it impossible to measure the shape of the same structure between different frames, resulting in partial overlap of the point clouds and reduced alignment accuracy. The reason why the measured area often changed because the amount of displacement of the robot in each frame was large and was greatly affected by the occlusion by the objects in the environment. The LiDAR used in experiment had a narrow angle of view in the pitch direction (30 degrees), and tilted during the measurement. This is another reason why the shape of the same structure could not be measured between different frames, since the height at which the laser hits the structure varies greatly as the robot displacement. To cope with these problems, it is important to increase the number of frames for measurement and to use LiDAR with a wide angle of view. In addition, it is also effective to adopt a method which can align partially overlapping point clouds.

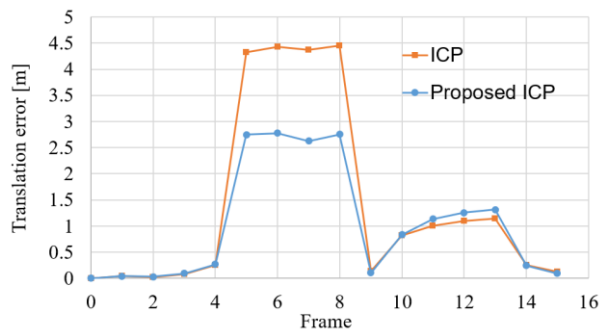


Fig. 9 Comparison of translation errors.

Table 3 Mean of translation errors [m]

ICP	1.410
Proposed ICP	1.021

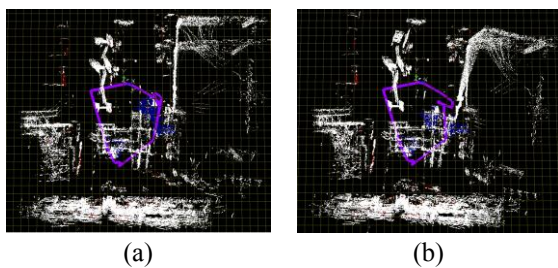


Fig. 10 Built map by (a) conventional ICP and (b) proposed ICP.

Table 4 Distance to the map build by true trajectory [m]

ICP	1.360
Proposed ICP	1.291

V. CONCLUSIONS

In this paper, we propose a method to generate an environmental map by applying LiDAR reflection intensity and water source measurements as characteristic physical quantities to ICP. In the proposed method, we constructed a SLAM system considering physical features by expanding the

search range by classes of physical features and adding a penalty for matching points of different classes in the nearest neighbor search in the ICP algorithm. In experiments, we used ICP with physical features to generate relatively accurate maps.

As a future work, we will address the problem of that the measured area often changed with the frames. In addition, other physical features such as temperature and polarization information, which have not been treated in this paper, are considered to be utilized in SLAM. Moreover, Since the advanced version of ICP treated in this paper has a problem that it is highly dependent on the initial alignment results, we also intend to consider an alignment method that focuses on global alignment, taking advantage of physical features.

REFERENCES

- [1] P. J. Besl and N. D. McKay, "A Method for Registration of 3D Shapes," *IEEE Transactions on Pattern Analysis and Machine Intelligence*, Vol. 8, No. 6, pp. 679–698, 1986.
- [2] D. Chetverikov, D. Svirko, D. Stepanov, and P. Krsek, "The Trimmed Iterative Closest Point Algorithm," *Proceedings of IEEE International Conference on Pattern Recognition*, pp. 545–548, 2002.
- [3] P. Biber and W. Strasser, "The Normal Distributions Transform: A New Approach to Laser Scan Matching," *Proceedings of the 2003 IEEE/RSJ International Conference on Intelligent Robots and Systems*, Vol. 3, pp. 2743–2748, 2003.
- [4] J. Engel, V. Koltun, and D. Cremers, "Direct Sparse Odometry," *IEEE Transactions on Pattern Analysis and Machine Intelligence*, Vol. 40, pp. 611–625, 2017.
- [5] R. Mur-Artal, J. M. M. Montiel, and J. D. Tardes, "ORB-SLAM: A Versatile and Accurate Monocular SLAM System," *IEEE Transactions on Robotics*, Vol. 31, No. 5, pp. 1147–1163, 2015.
- [6] M. Yokozuka, S. Oishi, S. Thompson, and A. Banno, "VITAMIN-E: Visual Tracking and Mapping with Extremely Dense Feature Points," *Proceedings of IEEE Conference on Computer Vision and Pattern Recognition*, pp. 9641–9650, 2019.
- [7] R. B. Rusu, N. Blodow, and M. Beetz, "Fast Point Feature Histograms (FPFH) for 3D registration," *Proceedings of the 2009 IEEE International Conference on Robotics and Automation*, pp. 3212–3217, 2009.
- [8] Y. Hara, H. Kawata, A. Ohya, and S. Yuta, "Mobile Robot Localization and Mapping by Scan Matching using Laser Reflection Intensity of the SOKUIKI Sensor," *Proceedings of the 32nd Annual Conference of the IEEE Industrial Electronics Society*, pp. 3018–3023, 2006.
- [9] G. Godin, D. Laurendeau, and R. Bergevin, "A Method for the Registration of Attributed Range Images," *Proceedings of the 2001 International Conference on 3D Imaging and Modeling*, pp. 179–86, 2001.
- [10] R. Kataoka, R. Suzuki, Y. Ji, H. Fujii, H. Kono, and K. Umeda, "SLAM Based on ICP and Loop Closing Considering Physical Properties of Environment," *Proceedings of 25th Robotics Symposia*, pp. 246–249, 2020. (in Japanese)
- [11] R. Suzuki, R. Kataoka, Y. Ji, H. Fujii, H. Kono, and K. Umeda, "SLAM Using ICP and Graph Optimization Considering Physical Properties of Environment," *arXiv:2007.00483*, 2020.
- [12] H. Fujii, M. Sugawara, H. Kono, and Y. Ji, "3D Visualization of Near-Infrared Information for Detecting Water Source," *Proceedings of Fukushima Research Conference on Remote Technologies for Nuclear Facilities 2019*, p. 5, 2019.